ELSEVIER

Journal of Organometallic Chemistry 569 (1998) 99–108

Journal of Organometallic Chemistry

# Synthesis and reactivities of the indenyl-ruthenium cluster $[(\eta^5\text{-}C_9H_7)Ru(\mu\text{-}SEt)]_3$: indenyl effect in the trinuclear ruthenium cluster[1]

Tetsu Sato [a], Masayuki Nishio [b], Youichi Ishii [b], Hiroshi Yamazaki [a], Masanobu Hidai [b,*]

[a] *Department of Applied Chemistry, Faculty of Science and Engineering, Chuo University, Kasuga, Bunkyo-ku, Tokyo 112-8551, Japan*
[b] *Department of Chemistry and Biotechnology, Graduate School of Engineering, The University of Tokyo, Hongo, Bunkyo-ku, Tokyo 113-8656, Japan*

Received 18 March 1998

**Abstract**

The triruthenium cluster with bridging ethanethiolato and indenyl ligands $[(\eta^5\text{-}C_9H_7)Ru(\mu\text{-}SEt)]_3$ (**2**) was synthesized by heating the mononuclear indenyl complex $[(\eta^5\text{-}C_9H_7)Ru(SEt)(PPh_3)_2]$ (**1a**) in toluene. Cluster **2** reacted with MeI to afford the S-methylated cluster $[(\eta^5\text{-}C_9H_7)_3Ru_3(\mu\text{-}SEt)_2(\mu\text{-}SEtMe)]I\cdot CH_2Cl_2$ (**4a**) with high stereoselectivity through the attack of MeI on the axial SEt group from the equatorial side. The $PF_6^-$ salt of the cationic cluster $[(\eta^5\text{-}C_9H_7)_3Ru_3(\mu\text{-}SEt)_2(\mu\text{-}SEtMe)][PF_6]$ was further converted into the cationic carbonyl complex $[(\eta^5\text{-}C_9H_7)_2Ru_2(\mu\text{-}SEt)(CO)_4][PF_6]$ (**5**) by treatment with CO at 50°C. The crystal structures of **4a** and **5** were determined by X-ray diffraction study. When a THF solution of **2** was allowed to contact with atmospheric pressure of CO at room temperature, the trinuclear carbonyl cluster $[(\eta^5\text{-}C_9H_7)_3Ru_3(\mu\text{-}SEt)_3(\mu\text{-}CO)(CO)]$ (**6**) and the dinuclear carbonyl complex $[(\eta^5\text{-}C_9H_7)Ru(\mu\text{-}SEt)(CO)]_2$ (**7**) were obtained. The structures of **6** and **7** were also crystallographically determined. Furthermore, cluster **2** was oxidized in refluxing $CHCl_3$ to give $[(\eta^5\text{-}C_9H_7)Ru(SEt)Cl]_n$ (**9**). The Cp analogue of **2**, $[CpRu(\mu\text{-}SEt)]_3$, failed to react with CO and $CHCl_3$, and the hapticity change of the indenyl ligand in **2** is considered to be crucial for the initial interaction of **2** with CO and $CHCl_3$. These reactions provide rare examples of the indenyl ligand effect in a multinuclear complex. 

*Keywords:* Ruthenium; Indenyl ligand; Thiolato ligand; Cluster; X-ray crystal structure

## 1. Introduction

The chemistry of sulfur-bridged multinuclear transition metal complexes is a subject under current scrutiny owing not only to their structural diversity [1] but also to their involvement in the active sites of metalloproteins [2] and relevance to the industrial hydrodesulfurization catalysts [3]. During the last decade we have been focusing our attention on syntheses and reactions of sulfur-bridged complexes of groups 8–10 noble metals [4]. Previously, we prepared a series of multinuclear sulfido, hydrosulfido, and thiolato complexes of ruthenium [5–7], which exhibited unique reactivities [8] and catalytic activities [9] characteristic of their multinuclear cores. Although considerable efforts have recently been devoted to the synthesis of ruthenium–sulfur multinuclear complexes by several groups [5–7,10], most of the compounds reported are those containing Cp, Cp*, and their simple alkyl analogues ($Cp = \eta^5\text{-}C_5H_5$, $Cp^* = \eta^5\text{-}C_5Me_5$). However, these ancillary ligands have a strong tendency to take a $\eta^5$-coordination mode, and it is often difficult to generate a vacant coordination site on the metal center by the ring slippage of the Cp or Cp* ligand. Intrigued by the

* Corresponding author.

[1] Dedicated to Professor Nakamura on the occasion of his retirement from Osaka University.

0022-328X/98/$ - see front matter 
*PII* S0022-328X(98)00778-5

possibility that use of the coordinatively more labile ancillary ligands than Cp and Cp* ligands in this class of complexes will lead to exploitation of their new reactivities, we set out to synthesize multinuclear ruthenium–sulfur complexes with indenyl ligands.

The indenyl ligand has been known to undergo more facile $\eta^5$ to $\eta^3$ ring slippage than the Cp and Cp* ligands due to the accompanying aromatization of the $C_6$ ring, providing a vacant coordination site necessary for further reactions [11]. By this effect, indenyl complexes are often endowed with higher reactivities in various types of ligand substitution and related reactions in comparison with the corresponding Cp analogues. Such 'indenyl ligand effect' has been attracting great interest in recent years and well documented with mononuclear complexes [12]. However, little has been investigated with the indenyl ligand effect in clusters [13]. In this paper, we describe synthesis of a thiolato-bridged trinuclear ruthenium cluster with indenyl ligands and its unique reactivities.

## 2. Results and discussion

### 2.1. Synthesis of the trinuclear indenyl cluster $[(\eta^5\text{-}C_9H_7)Ru(\mu\text{-}SEt)]_3$

Although our attempts to synthesize thiolato-bridged dinuclear ruthenium complexes with indenyl ligands were unfruitful, we succeeded in synthesizing the triruthenium cluster with indenyl and bridging ethanethiolato ligands, $[(\eta^5\text{-}C_9H_7)Ru(\mu\text{-}SEt)]_3$ (**2**). Thus, the mononuclear indenyl complex $[(\eta^5\text{-}C_9H_7)Ru(SEt)(PPh_3)_2]$ (**1a**) was first prepared from $[(\eta^5\text{-}C_9H_7)RuCl(PPh_3)_2]$ by treatment with excess amounts of NaSEt in refluxing THF. Heating a toluene solution of complex **1a** under reflux gave cluster **2** as a dark purple microcrystalline solid in good yield with the dissociation of $PPh_3$.

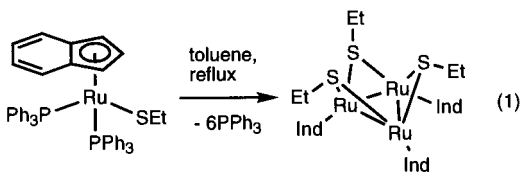


**1a** **2**

[Ind = $\eta^5$-$C_9H_7$]

A similar method was already reported by Shaver and co-workers for the synthesis of the analogous Cp clusters $[CpRu(\mu\text{-}SR)]_3$ (R = $^n$Pr, $^i$Pr) [14]. However, reactions of some other alkane and arenethiolato complexes $[(\eta^5\text{-}C_9H_7)Ru(SR)(PPh_3)_2]$ (**1b**, R = $^i$Pr; **1c**, R = $CH_2Ph$; **1d**, R = 4-$MeC_6H_4$) under similar conditions ended in the formation of a complex mixture.

Cluster **2** is highly soluble in most common organic solvents including hexane and was characterized spectroscopically. The $^1$H-NMR spectrum of **2** exhibited two distinct sets of signals in the ratio of 2:1 for each of the indenyl and SEt groups. The SEt signal with the larger relative intensity appeared as an $ABX_3$ pattern ($\delta$ 1.12 (t, 6H), 2.00 (dq, 2H), 2.02 (dq, 2H)) indicating the diastereotopic nature of the methylene protons, while the other SEt signal was observed as a common $A_2X_3$ pattern ($\delta$ 0.84 (t, 3H), 2.47 (q, 2H)). Similarly, the set of the indenyl signals with the larger relative intensity ($\delta$ 4.61 (m, 2H), 4.69 (m, 2H), 4.94 (t, 2H)) revealed that these indenyl ligands are located in unsymmetric circumstances. These $^1$H-NMR features, as well as the analytical data, suggest that complex **2** has a triangular $Ru_3$ core with one bridging SEt ligand on each edge, where two of the SEt groups occupy equatorial positions with respect to the chair-like $Ru_3S_3$ ring, and the third SEt group takes axial conformation (Eqn. 1). This type of structure was also found in the related Cp cluster $[CpRu(\mu\text{-}S^nPr)]_3$ (**3**) [14]. Assuming that the structure of cluster **2** is analogous to that of **3**, the 48e$^-$ core of **2** has three Ru–Ru bonds. The molecular structure of **2** was further supported by the diffraction study of the S-methylation product from **2** (vide infra).

### 2.2. Reaction of $[(\eta^5\text{-}C_9H_7)Ru(\mu\text{-}SEt)]_3$ with MeI

We have previously reported that the thiolato-bridged Ru(II)–Ru(II) dinuclear complex $[Cp^*Ru(\mu\text{-}S^iPr)_2RuCp^*]$ undergoes oxidative addition with alkyl halides (RX) at the dinuclear center to give the corresponding Ru(III)–Ru(III) complex $[Cp^*RuR(\mu\text{-}S^iPr)_2RuXCp^*]$ [7]. In contrast, the reaction of the trinuclear cluster **2** with MeI afforded the S-methylated cationic cluster $[(\eta^5\text{-}C_9H_7)_3Ru_3(\mu\text{-}SEt)_2(\mu\text{-}SEtMe)]I$ (**4a**) in good yield[2].

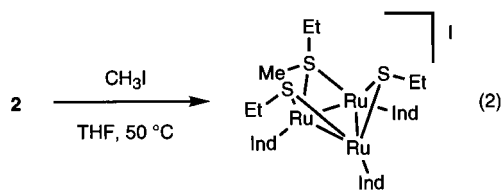


**4a**

This result is comparable with the reaction of the Ir(II)–Ir(II) complex $[Cp^*Ir(\mu\text{-}SR)_2IrCp^*]$ (R = $^i$Pr, cyclohexyl) with MeOTf (OTf = $OSO_2CF_3$), which yielded the S-methylated complex $[Cp^*Ir(\mu\text{-}SR)(\mu\text{-}SMeR)IrCp^*][OTf]$ [15]. In complexes **2** and $[Cp^*Ir(\mu\text{-}SR)_2IrCp^*]$ each metal center satisfies the effective atomic number of 18e$^-$ by making two or one metal–

[2] Similar S-methylation was also observed with $[CpRu(\mu\text{-}SEt)]_3$. $[Cp_3Ru_3(\mu\text{-}SEt)_2(\mu\text{-}SEtMe)]I\cdot CH_2Cl_2$: yield 19%, $^1$H-NMR ($CDCl_3$) $\delta$ 1.15 (t, 6H, $J$ = 7.3 Hz, $SCH_2\mathit{Me}$), 1.44–1.65 (m, 4H, $SCH_2Me$), 1.57 (t, 3H, $J$ = 7.3 Hz, $MeSCH_2\mathit{Me}$), 2.58 (s, 3H, $SCH_3$), 3.71 (q, 2H, $J$ = 7.3 Hz, $MeSCH_2Me$), 5.03 (s, 5H, $\eta^5$-$C_5H_5$), 5.17 (s, 10H, $\eta^5$-$C_5H_5$).

Table 1
Selected bond distances and angles for $[(\eta^5\text{-}C_9H_7)_3Ru_3(\mu\text{-}SEt)_2(\mu\text{-}SEtMe)]I\cdot CH_2Cl_2$ (**4a**$\cdot CH_2Cl_2$)

| | | | |
|---|---|---|---|
| Distances (Å) | | | |
| Ru(1)–Ru(2) | 2.741(1) | Ru(1)–Ru(3) | 2.728(1) |
| Ru(2)–Ru(3) | 2.753(1) | Ru(1)–S(1) | 2.296(2) |
| Ru(1)–S(2) | 2.280(2) | Ru(2)–S(2) | 2.295(2) |
| Ru(2)–S(3) | 2.259(2) | Ru(3)–S(1) | 2.304(2) |
| Ru(3)–S(3) | 2.256(2) | Ru(1)–C(1) | 2.401(8) |
| Ru(1)–C(2) | 2.213(8) | Ru(1)–C(3) | 2.164(7) |
| Ru(1)–C(4) | 2.189(8) | Ru(1)–C(5) | 2.402(8) |
| Ru(2)–C(10) | 2.309(8) | Ru(2)–C(11) | 2.197(8) |
| Ru(2)–C(12) | 2.176(8) | Ru(2)–C(13) | 2.207(8) |
| Ru(2)–C(14) | 2.328(8) | Ru(3)–C(19) | 2.347(8) |
| Ru(3)–C(20) | 2.178(7) | Ru(3)–C(21) | 2.174(7) |
| Ru(3)–C(22) | 2.206(7) | Ru(3)–C(23) | 2.322(7) |
| Angles (°) | | | |
| Ru(1)–Ru(2)–Ru(3) | 59.53(2) | Ru(2)–Ru(1)–Ru(3) | 60.46(2) |
| Ru(1)–Ru(3)–Ru(2) | 60.01(3) | S(1)–Ru(1)–S(2) | 81.98(7) |
| S(2)–Ru(2)–S(3) | 88.26(7) | S(1)–Ru(3)–S(3) | 90.48(7) |
| Ru(1)–S(1)–Ru(3) | 72.73(6) | Ru(1)–S(2)–Ru(2) | 73.61(7) |
| Ru(2)–S(3)–Ru(3) | 75.15(6) | | |

metal bonds, respectively, while the complex [Cp*Ru($\mu$-S$^i$Pr)$_2$RuCp*] has two coordinatively unsaturated (16e$^-$) ruthenium centers. The difference in the electronic structure between **2** and [Cp*Ru($\mu$-S$^i$Pr)$_2$RuCp*] is probably reflected in the reactivities toward MeI.

The $^1$H-NMR spectrum of cluster **4a** exhibited a new SMe singlet at $\delta$ 2.94 in addition to the SEt and indenyl signals similar to those described for cluster **2**. Other spectral and analytical data are also consistent with the formulation in Eqn. 2. The molecular structure of **4a** was unambiguously determined by X-ray crystallography. Selected bond distances and angles are listed in Table 1, and an ORTEP drawing is depicted in Fig. 1.

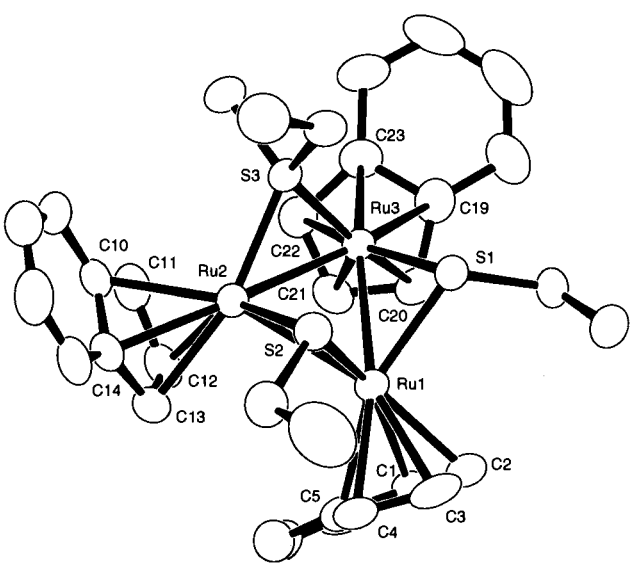


Fig. 1. An ORTEP drawing of the cationic part in $[(\eta^5\text{-}C_9H_7)_3Ru_3(\mu\text{-}SEt)_2(\mu\text{-}SEtMe)]I\cdot CH_2Cl_2$ (**4a**$\cdot CH_2Cl_2$).

In agreement with the formulation, cluster **4a** is a triangular cluster with two $\mu$-SEt and one $\mu$-SEtMe ligands. The sulfur atoms are coordinated in mutually *cis* configuration with respect to the $Ru_3$ plane. The Ru–Ru distances (2.728–2.753 Å) are indicative of the presence of three Ru–Ru single bonds among the three ruthenium atoms, being in accordance with the 48 valence electrons of **4a**. The three indenyl ligands are also mutually *cis*. The slip values ($\Delta_{M-C}$, 0.117–0.201 Å), the hinge angles (HA, 3.8–5.9°), and the fold angles (FA, 4.1–10.9°) found in **4a** are diagnostic of $\eta^5$ coordination of the indenyl ligands.[3] The Et group of the SEtMe ligand is located in the axial position, while the other SEt and SMe groups occupy the equatorial positions. These crystallographic results also strongly support the spectroscopically characterized structure of cluster **2**.

Judging from the molecular structure, cluster **4a** was formed through the attack of MeI on the axial SEt group from the equatorial side of **2**. Interestingly, the $^1$H-NMR analysis of the crude reaction mixture revealed that no other stereoisomer than **4a** is produced during the reaction, indicating that the S-methylation of **2** proceeds with very high stereoselectivity. This selectivity can be accounted for by considering that the axial SEt group is situated close to the lone pair on the other bridging sulfur atoms and protects these sulfur atoms effectively from attack by MeI from the axial side. In fact, it has been reported that, in the molecular structure of **3**, one of the $\alpha$-protons of the axial S$^n$Pr group is within the van der Waals contact distance of the other sulfur atoms [14].

When the cationic indenyl cluster $[(\eta^5\text{-}C_9H_7)_3Ru_3(\mu\text{-}SEt)_2(\mu\text{-}SEtMe)][PF_6]$ (**4b**), which was prepared by anion metathesis of **4a** with $KPF_6$, was allowed to react with CO at 50°C for 55 h, a new cationic carbonyl complex $[(\eta^5\text{-}C_9H_7)_2Ru_2(\mu\text{-}SEt)(CO)_4][PF_6]$ (**5**) was obtained in moderate yield.

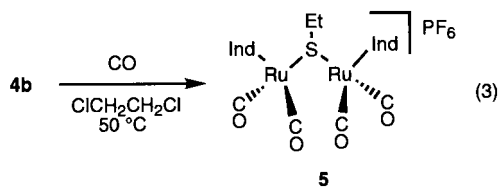


The $^1$H-NMR spectrum of **5** revealed that it contains two equivalent indenyl ligands and one SEt ligand, and

[3] $\Delta_{M-C}$ for **4a** represents [M–C$_{av}$(for C(1),C(5))] – [M–C$_{av}$(for C(2),C(4))], [M–C$_{av}$(for C(10), C(14))] – [M–C$_{av}$(for C(11),C(13))], and [M–C$_{av}$(for C(l9),C(23))]–[M–C$_{av}$(for C(20),C(22))]. HA represents the bending of the indenyl ligands at C(2)/C(4), C(11)/C(13), and C(20)/C(22), and FA at C(1)/C(5), C(10)/C(14), and C(19)/C(23) [16].

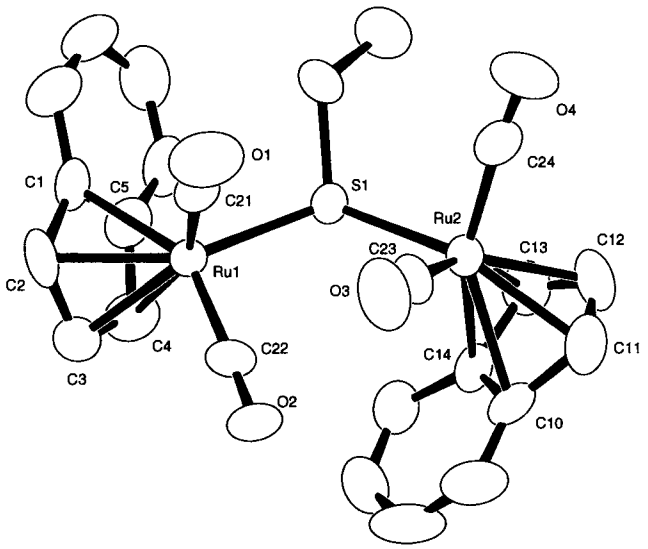


Fig. 2. An ORTEP drawing of the cationic part in $[(\eta^5\text{-}C_9H_7)_2Ru_2(\mu\text{-}SEt)(CO)_4][PF_6]$ (**5**).

the IR spectrum exhibited four absorptions due to terminally bound CO ligands at 1991, 2010, 2037 and 2058 $cm^{-1}$. The molecular structure of **5** was further confirmed by X-ray diffraction study. An ORTEP drawing is depicted in Fig. 2, and selected bond distances and angles are given in Table 2. Complex **5** consists of two $(\eta^5\text{-}C_9H_7)Ru(CO)_2$ moieties linked by a $\mu$-SEt bridge. The Ru–Ru separation at 4.166(1) Å excludes the presence of any bonding interaction between the two ruthenium atoms.

### 2.3. Reaction of $[(\eta^5\text{-}C_9H_7)Ru(\mu\text{-}SEt)]_3$ with CO

When a THF solution of cluster **2** was allowed to contact with atmospheric pressure of CO at room temperature, the starting **2** was consumed within 1 h, and

Table 2
Selected bond distances and angles for $[(\eta^5\text{-}C_9H_7)_2Ru_2(\mu\text{-}SEt)(CO)_4][PF_6]$ (**5**)

| | | | |
|---|---|---|---|
| Distances (Å) | | | |
| Ru(1)···Ru(2) | 4.166(1) | Ru(1)–S(1) | 2.392(3) |
| Ru(2)–S(1) | 2.408(3) | Ru(1)–C(1) | 2.316(9) |
| Ru(1)–C(2) | 2.191(9) | Ru(1)–C(3) | 2.181(9) |
| Ru(1)–C(4) | 2.216(9) | Ru(1)–C(5) | 2.362(10) |
| Ru(1)–C(21) | 1.90(1) | Ru(1)–C(22) | 1.837(10) |
| Ru(2)–C(10) | 2.335(9) | Ru(2)–C(11) | 2.21(1) |
| Ru(2)–C(12) | 2.22(1) | Ru(2)–C(13) | 2.23(1) |
| Ru(2)–C(14) | 2.331(9) | Ru(2)–C(23) | 1.89(1) |
| Ru(2)–C(24) | 1.87(1) | | |
| Angles (°) | | | |
| Ru(1)–S(1)–Ru(2) | 120.4(1) | S(1)–Ru(1)–C(21) | 91.4(3) |
| S(1)–Ru(1)–C(22) | 96.5(3) | S(1)–Ru(2)–C(23) | 95.5(3) |
| S(1)–Ru(2)–C(24) | 94.4(3) | | |

the trinuclear carbonyl cluster $[(\eta^5\text{-}C_9H_7)_3Ru_3(\mu\text{-}SEt)_3(\mu\text{-}Co)(CO)]$ (**6**) and the dinuclear carbonyl complex $[(\eta^5\text{-}C_9H_7)Ru(\mu\text{-}SEt)(CO)]_2$ (**7**) were isolated from the reaction mixture by chromatographic separation.

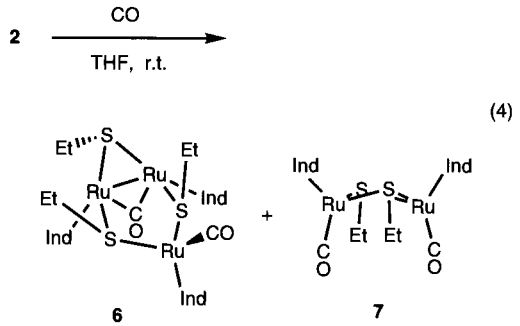


Both of the two compounds were characterized spectroscopically as well as crystallographically.

Similarly to cluster **2**, cluster **6** showed two sets of $^1$H-NMR signals with the relative intensity of 2:1 for each of the SEt and indenyl protons, suggesting that the trinuclear core of **2** is maintained in **6**. The IR spectra revealed that cluster **6** contains a terminal ($\nu_{CO}$, 1927 $cm^{-1}$) and a bridging ($\nu_{CO}$, 1748 $cm^{-1}$) carbonyl ligand. The crystal structure of **6** is fully consistent with these spectral data.

The unit cell in the crystal of **6** contained two crystallographically independent molecules. ORTEP drawings for the independent molecules of cluster **6** are given in Fig. 3, and selected bond distances and angles are in Table 3. The two molecules are significantly different in the orientation of the indenyl ligands, but the structures of the $Ru_3(\mu\text{-}SEt)_3(\mu\text{-}CO)(CO)$ cores are essentially equivalent except for the slight difference in the nonbonding Ru–Ru distances. Cluster **6** is composed of three $(\eta^5\text{-}C_9H_7)Ru$ fragments bridged by three SEt ligands, and two of the ruthenium atoms are also bridged by a CO ligand, while the third ruthenium center binds a terminal CO ligand. The two CO ligands are mutually *trans* with respect to the $Ru_3$ plane. The doubly bridged Ru–Ru contact in each molecule (2.7163(6), 2.7159(6) Å) corresponds to a Ru–Ru single bond. The other Ru–Ru distances (4.1179–4.1998 Å) are significantly long and demonstrate that two of the three Ru–Ru bonds in **2** are cleaved on incorporation of two CO molecules. The SEt group at the Ru–Ru single bond in **6** is oriented in an equatorial-like position, and the other SEt groups axial. This conformation is in contrast to the equatorial–equatorial–axial conformation of SEt groups found in **2**. It should also be pointed out that the Cp analogues of cluster **6** $[Cp_3Ru_3(\mu\text{-}SR)_3(\mu\text{-}CO)(CO)]$ (R = Me, Ph) were prepared by irradiation of $[CpRu(SR)(CO)_2]$, but their molecular structures have not been known [17]. These complexes are presumed to have the structures similar (or stereoisomeric) to that found for **6**.

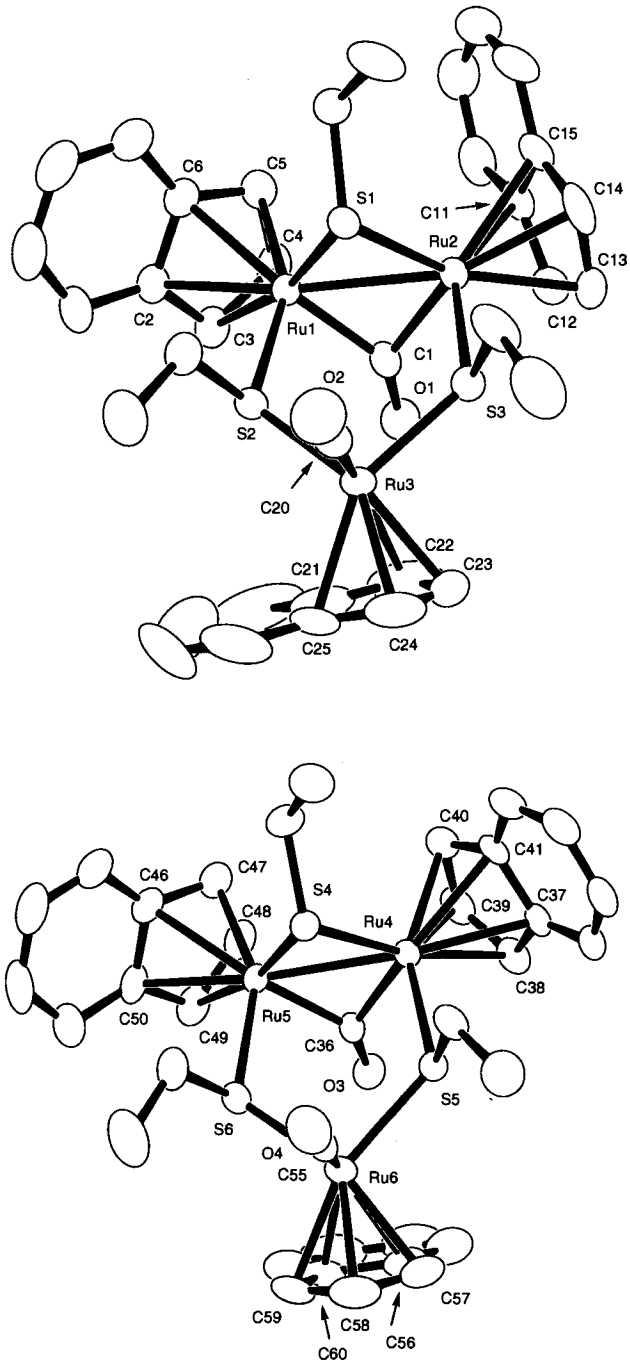


Fig. 3. ORTEP drawings of two independent molecules in the unit cell of $[(\eta^5\text{-}C_9H_7)_3Ru_3(\mu\text{-}SEt)_3(\mu\text{-}CO)(CO)]$ (**6**).

The molecular structure of the dinuclear carbonyl complex **7** is shown in Fig. 4, and selected bond distances and angles are listed in Table 4. Complex **7** has two $(\eta^5\text{-}C_9H_7)Ru(CO)$ fragments bridged by two SEt ligands, where the SEt groups adopt *syn* configuration, and both the indenyl and CO ligands are *cis* to each other. The $Ru_2S_2$ core is puckered with a dihedral angle of 162.5° around the Ru–Ru axis. There is no bonding interaction between the two ruthenium atoms (Ru(1)–Ru(2), 3.6412(8) Å). The $^1$H-NMR spectrum was in full agreement with this solid state structure, showing the $\eta^5$-indenyl ($\delta$ 4.39, t; 4.72, d) and SEt resonances ($\delta$ 1.05, t; 2.54, q). The structural and spectral features observed for **7** are comparable to related Cp* complexes such as $[Cp^*Ru(\mu\text{-}S^tBu)(CO)]_2$ [18] and $[Cp^*Fe(\mu\text{-}SEt)(CO)]_2$ [19].

In order to compare the reactivities of cluster **2** and its Cp analogue $[CpRu(\mu\text{-}SEt)]_3$ (**8**), reaction of **8** with CO was also examined. As expected, cluster **8** was recovered unchanged even after stirring for 3 days at room temperature. The much higher reactivity of cluster **2** is obviously ascribed to the presence of the indenyl ligands, and we consider that the hapticity change of an

Table 3
Selected bond distances and angles for $[(\eta^5\text{-}C_9H_7)_3Ru_3(\mu\text{-}SEt)_3(\mu\text{-}CO)(CO)]$ (**6**)

| | | | |
|---|---|---|---|
| Distances (Å) | | | |
| Ru(1)–Ru(2) | 2.7163(6) | Ru(1)···Ru(3) | 4.1183(9) |
| Ru(2)···Ru(3) | 4.1179(7) | Ru(1)–S(1) | 2.334(1) |
| Ru(1)–S(2) | 2.374(1) | Ru(2)–S(1) | 2.321(1) |
| Ru(2)–S(3) | 2.346(1) | Ru(3)–S(2) | 2.372(1) |
| Ru(3)–S(3) | 2.359(1) | Ru(1)–C(1) | 1.981(4) |
| Ru(1)–C(2) | 2.305(4) | Ru(1)–C(3) | 2.197(4) |
| Ru(1)–C(4) | 2.170(4) | Ru(1)–C(5) | 2.206(4) |
| Ru(1)–C(6) | 2.334(4) | Ru(2)–C(1) | 2.025(4) |
| Ru(2)–C(11) | 2.378(4) | Ru(2)–C(12) | 2.224(4) |
| Ru(2)–C(13) | 2.192(4) | Ru(2)–C(14) | 2.216(4) |
| Ru(2)–C(15) | 2.388(4) | Ru(3)–C(20) | 1.849(5) |
| Ru(3)–C(21) | 2.348(5) | Ru(3)–C(22) | 2.275(6) |
| Ru(3)–C(23) | 2.220(6) | Ru(3)–C(24) | 2.188(5) |
| Ru(3)–C(25) | 2.282(5) | | |
| Ru(4)–Ru(5) | 2.7159(6) | Ru(4)···Ru(6) | 4.1998(7) |
| Ru(5)···Ru(6) | 4.1777(8) | Ru(4)–S(4) | 2.342(1) |
| Ru(4)–S(5) | 2.390(1) | Ru(5)–S(4) | 2.331(1) |
| Ru(5)–S(6) | 2.394(1) | Ru(6)–S(5) | 2.401(1) |
| Ru(6)–S(6) | 2.384(1) | Ru(4)–C(36) | 2.004(4) |
| Ru(4)–C(37) | 2.316(4) | Ru(4)–C(38) | 2.203(4) |
| Ru(4)–C(39) | 2.184(4) | Ru(4)–C(40) | 2.224(4) |
| Ru(4)–C(41) | 2.331(4) | Ru(5)–C(36) | 1.997(4) |
| Ru(5)–C(46) | 2.327(4) | Ru(5)–C(47) | 2.202(4) |
| Ru(5)–C(48) | 2.178(4) | Ru(5)–C(49) | 2.198(4) |
| Ru(5)–C(50) | 2.313(4) | Ru(6)–C(55) | 1.800(5) |
| Ru(6)–C(56) | 2.393(5) | Ru(6)–C(57) | 2.231(4) |
| Ru(6)–C(58) | 2.175(4) | Ru(6)–C(59) | 2.213(4) |
| Ru(6)–C(60) | 2.378(4) | | |
| Angles (°) | | | |
| Ru(2)–Ru(1)–S(2) | 99.98(3) | Ru(1)–Ru(2)–S(3) | 99.40(3) |
| S(1)–Ru(1)–S(2) | 86.26(4) | S(1)–Ru(2)–S(3) | 86.64(4) |
| S(2)–Ru(3)–S(3) | 95.81(4) | S(2)–Ru(1)–C(1) | 86.0(1) |
| S(3)–Ru(2)–C(1) | 85.3(1) | S(2)–Ru(3)–C(20) | 93.8(1) |
| S(3)–Ru(3)–C(20) | 94.9(1) | Ru(1)–S(1)–Ru(2) | 71.39(3) |
| Ru(1)–S(2)–Ru(3) | 120.39(5) | Ru(2)–S(3)–Ru(3) | 122.15(5) |
| Ru(1)–C(1)–Ru(2) | 85.4(2) | | |
| Ru(5)–Ru(4)–S(5) | 99.18(3) | Ru(4)–Ru(5)–S(6) | 100.05(3) |
| S(4)–Ru(4)–S(5) | 87.89(4) | S(4)–Ru(5)–S(6) | 87.55(4) |
| S(5)–Ru(6)–S(6) | 94.57(4) | S(5)–Ru(4)–C(36) | 85.1(1) |
| S(6)–Ru(5)–C(36) | 86.4(1) | S(5)–Ru(6)–C(55) | 92.8(1) |
| S(6)–Ru(6)–C(55) | 94.7(1) | Ru(4)–S(4)–Ru(5) | 71.06(3) |
| Ru(4)–S(5)–Ru(6) | 122.48(4) | Ru(5)–S(6)–Ru(6) | 121.93(4) |
| Ru(4)–C(36)–Ru(5) | 85.5(2) | | |

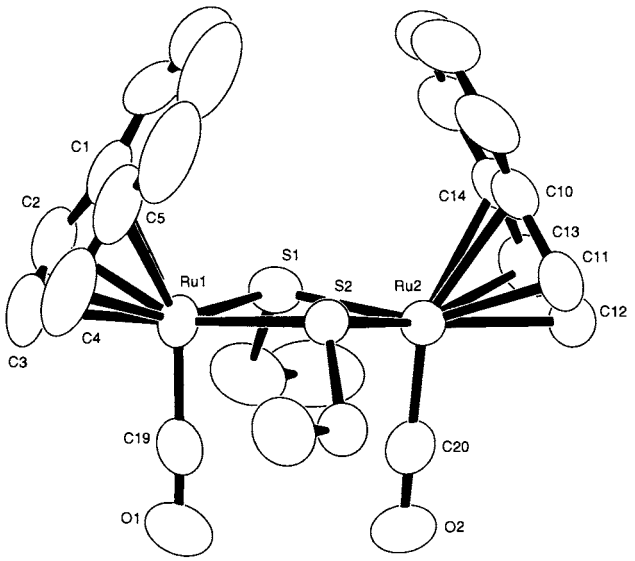


Fig. 4. An ORTEP drawing of $[(\eta^5\text{-}C_9H_7)Ru(\mu\text{-}SEt)(CO)]_2$ (**7**).

indenyl ligand from $\eta^5$- to $\eta^3$-mode is essential for the initial CO incorporation onto the cluster core. Based on these observations, a proposed mechanism for the formation of **6** from **2** is illustrated in Scheme 1. The reaction is initiated by isomerization of an $\eta^5$-indenyl ligand into the $\eta^3$-mode followed by the coordination of a CO molecule to the vacant site generated. Isomerization of the $\eta^3$-indenyl ligand back to the $\eta^5$-mode is accompanied by the cleavage of the two Ru–Ru bonds. Considering the axial–axial–equatorial conformation of the SEt groups found in **6**, inversion of the chair-like conformation of the $Ru_3S_3$ six-membered ring should also take place during the above process. Finally, another CO molecule reacts with the unsaturated Ru=Ru moiety to produce the final product **6**. Since neither complex **6** nor **7** underwent any further reaction with CO at room temperature in THF, complexes **6** and **7** are supposed to be formed independently from **2** and

Table 4
Selected bond distances and angles for **7**

| | | | |
|---|---|---|---|
| Distances (Å) | | | |
| Ru(1)–Ru(2) | 3.6412(8) | Ru(1)–S(1) | 2.377(2) |
| Ru(1)–S(2) | 2.384(1) | Ru(2)–S(1) | 2.382(2) |
| Ru(2)–S(2) | 2.381(2) | Ru(1)–C(1) | 2.341(7) |
| Ru(1)–C(2) | 2.213(6) | Ru(1)–C(3) | 2.177(6) |
| Ru(1)–C(4) | 2.222(7) | Ru(1)–C(5) | 2.342(8) |
| Ru(1)–C(19) | 1.792(6) | Ru(2)–C(10) | 2.347(6) |
| Ru(2)–C(11) | 2.214(6) | Ru(2)–C(12) | 2.163(6) |
| Ru(2)–C(13) | 2.214(6) | Ru(2)–C(14) | 2.362(6) |
| Ru(2)–C(20) | 1.794(6) | | |
| Angles (°) | | | |
| S(1)–Ru(1)–S(2) | 79.15(5) | S(1)–Ru(2)–S(2) | 79.12(5) |
| S(1)–Ru(1)–C(19) | 94.7(2) | S(2)–Ru(1)–C(19) | 92.0(2) |
| S(1)–Ru(2)–C(20) | 92.4(2) | S(2)–Ru(2)–C(20) | 94.4(2) |
| Ru(1)–S(1)–Ru(2) | 99.83(6) | Ru(1)–S(2)–Ru(2) | 99.66(5) |

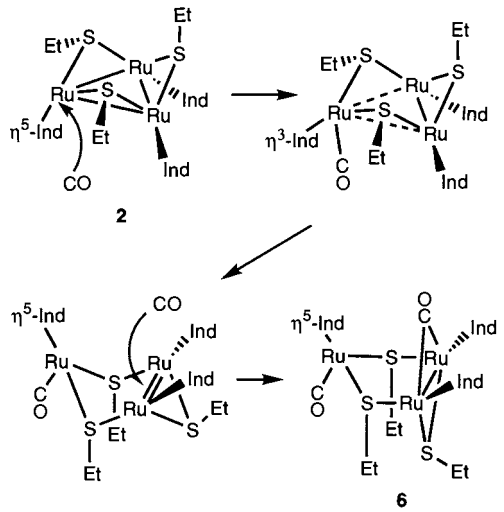


Scheme 1.

CO. However, we must await further investigation to elucidate the mechanism for the formation of dinuclear complex **7**. In any event, the reaction of cluster **2** with CO is interesting in that it provides a rare example of the indenyl ligand effect appeared in a multinuclear complex.

### 2.4. Reaction of $[(\eta^5\text{-}C_9H_7)Ru(\mu\text{-}SEt)]_3$ with $CHCl_3$

Oxidation of cluster **2** took place on refluxing in $CHCl_3$ for 2 h, and a dark red Ru(III) complex formulated as $[(\eta^5\text{-}C_9H_7)Ru(SEt)Cl]_n$ (**9**) was isolated in 14% yield.

$$\mathbf{2} \xrightarrow[\text{reflux}]{CHCl_3} [(\eta^5\text{-}C_9H_7)Ru(SEt)Cl]_n \qquad (5)$$

Complex **9** was essentially the only diamagnetic product detected by $^1$H-NMR analysis of the crude reaction mixture. The characterization of **9** is based on its $^1$H-NMR spectra exhibiting one set of indenyl and SEt resonances and satisfactory analytical data (C, H, S, and Cl). The diamagnetism and high symmetry revealed by the $^1$H-NMR analysis seem to suggest that complex **9** has a dimeric structure ($n = 2$). A related Ru(III)–Ru(III) dinuclear complex [Cp*RuCl($\mu$-SEt)$_2$RuCp*Cl] was previously prepared and found to show similar $^1$H-NMR features due to its *cis–syn* structure [6].

In contrast, the reaction of the Cp analogue **8** in refluxing $CHCl_3$ was found to be sluggish. The conversion was only 13% after 4 h, and an oxidation product similar to **9** could not be isolated. In order to gain insight into the difference in the reactivity, electrochemical properties of clusters **2** and **8** were compared. Interestingly, cyclic voltammogram measurements revealed that each of the clusters **2** and **8** has a reversible oxidation wave, where the oxidation potential of **2**

($E_{1/2} = 0.30$ V vs SCE, in $CH_2Cl_2$-0.1 M $NBu_4BF_4$) is slightly higher than that of **8** ($E_{1/2} = 0.20$ V). The discrepancy between the oxidation potentials and the susceptibility to the oxidation by $CHCl_3$ may be explained by the indenyl ligand effect in cluster **2**. Although the reaction mechanism has not been clarified, the $\eta^5-\eta^3$ isomerization of an indenyl ligand in **2** would play an important role in an early stage of the oxidation process.

In conclusion, we have prepared a novel trinuclear ruthenium cluster **2** with $\eta^5$-indenyl and bridging thiolato ligands and demonstrated that this cluster shows several interesting reactivities toward MeI, CO, and $CHCl_3$. In particular, the latter two reactions were not observed with the corresponding Cp cluster **8**, thus providing rare examples showing the indenyl ligand effect in a multinuclear complex.

## 3. Experimental section

### 3.1. General methods

All manipulations were carried out using standard Schlenk tube techniques. [($\eta^5$-$C_9H_7$)RuCl($PPh_3$)$_2$] [20] and [($\eta^5$-$C_5H_5$)RuCl($PPh_3$)$_2$] [21] were prepared according to literature methods. Sodium thiolates were prepared from the corresponding thiols and NaH. Solvents were dried and distilled prior to use. Alumina for column chromatography was purchased from Nacalai Tesque (Alumina Activated 200). Other reagents were commercially obtained and used without further purification. IR spectra were recorded on a Shimadzu 8100M spectrometer, while $^1$H- and $^{31}$P{$^1$H}-NMR spectra were obtained on a JEOL EX-270 spectrometer. Elemental analyses were carried out on a Perkin-Elmer 2400II CHN analyzer. Electrochemical measurements were made with Hokuto Denko instrumentation (HA-501 potentiostat and HB-105 function generator) by using a glassy carbon working electrode; potentials were measured in $CH_2Cl_2$-0.1 M [$Bu_4N$][$BF_4$] versus an SCE.

### 3.2. Preparation of [($\eta^5$-$C_9H_7$)Ru(SR)($PPh_3$)$_2$] (R = Et (**1a**), $^i$Pr (**1b**), $CH_2Ph$ (**1c**), 4-$MeC_6H_4$ (**1d**))

The following procedure for the preparation of **1a** (R = Et) is representative. To an orange solution of [($\eta^5$-$C_9H_7$)RuCl($PPh_3$)$_2$] (498 mg, 0.642 mmol) in THF (35 ml) was added NaSEt (223 mg, 2.66 mmol), and the mixture was allowed to reflux for 15 min. Rapid color change from orange to purple was observed. The solvent was removed in vacuo, and the resulting dark green solid was extracted with toluene. Addition of MeOH to the concentrated extract gave **1a**·MeOH as dark green crystals (395 mg, 0.474 mmol, 74%). $^1$H-NMR ($C_6D_6$):$\delta$ 1.69 (t, 3H, $J = 7.4$ Hz, $SCH_2Me$), 2.57 (q, 2H, $J = 7.4$ Hz, $SCH_2$Me), 4.36 (d, 2H, $J = 2.0$ Hz, $\eta^5$-$C_9H_7$), 5.26 (t, 1H, $J = 2.0$ Hz, $\eta^5$-$C_9H_7$), 6.94–7.52 (m, 34H, aryl); $^{31}$P{$^1$H}-NMR ($C_6D_6$): $\delta$ 49.88 (s). Anal. Calc. for $C_{48}H_{46}OP_2SRu$: C, 69.13; H, 5.56. Found: C, 69.32; H, 5.58.

**1b**, **1c**, and **1d** were prepared by similar procedures from [($\eta^5$-$C_9H_7$)RuCl($PPh_3$)$_2$] and NaS$^i$Pr, $NaSCH_2Ph$, and NaS(4-$MeC_6H_4$), respectively.

**1b**: Dark green crystals from toluene-MeOH (77%). $^1$H-NMR ($C_6D_6$): $\delta$ 1.71 (d, 6H, $J = 6.5$ Hz, $SCHMe_2$), 2.70 (sep, 1H, $J = 6.5$ Hz, $SCHMe_2$), 4.54 (br, 2H, [($\eta^5$-$C_9H_7$), 5.20 (br, 1H, $\eta^5$-$C_9H_7$), 6.90–7.83 (m, 34H, aryl); $^{31}$P{$^1$H}-NMR ($C_6D_6$): $\delta$ 48.38 (s). Anal. Calc. for $C_{48}H_{44}P_2SRu$: C, 70.66; H, 5.44. Found: C, 70.39; H, 5.65.

**1c**: Dark green crystals from toluene-MeOH (75%). $^1$H-NMR ($C_6D_6$): $\delta$ 3.72 (s, 2H, $SCH_2Ph$), 4.44 (d, 2H, $J = 2.5$ Hz, $\eta^5$-$C_9H_7$), 5.27 (br, 1H, $\eta^5$-$C_9H_7$), 6.89–7.48 (m, 39H, aryl); $^{31}$P{$^1$H}-NMR ($C_6D_6$): $\delta$ 50.14 (s). Anal. Calc. for $C_{52}H_{44}P_2SRu$: C, 72.29; H, 5.13. Found: C, 71.97; H, 5.06.

**1d**: Dark green crystals from toluene-MeOH (82%). $^1$H-NMR ($C_6D_6$): $\delta$ 2.29 (s, 3H, Me), 4.20 (d, 2H, $J = 2.0$ Hz, $\eta^5$-$C_9H_7$), 5.30 (t, 1H, $J = 2.0$ Hz, $\eta^5$-$C_9H_7$), 6.91–7.75 (m, 38H, aryl); $^{31}$P{$^1$H}-NMR ($C_6D_6$): $\delta$ 47.88 (s). Anal. Calc. for $C_{52}H_{44}P_2SRu$: C, 72.29; H, 5.13. Found: C, 72.15; H, 5.17.

### 3.3. Preparation of [($\eta^5$-$C_9H_7$)Ru($\mu$-SEt)]$_3$ (**2**)

A dark green solution of **1a** (253 mg, 0.315 mmol) in toluene (20 ml) was stirred at 100°C for 2 days. The purple brown solid obtained by evaporation of the solvent under reduced pressure was dissolved in toluene/hexane (1/1) and loaded on an activated alumina column. The column was washed with toluene/hexane (1/1) to remove $PPh_3$, and then a dark purple band eluted with toluene was collected. The eluate was dried up, and the residue was recrystallized from THF-MeOH to give **2** as a dark purple microcrystalline solid (45.2 mg, 0.0543 mmol, 52%). $^1$H-NMR ($C_6D_6$): $\delta$ 0.84 (t, 3H, $J = 7.3$ Hz, $SCH_2Me$), 1.12 (t, 6H, $J = 7.5$ Hz, $SCH_2Me$), 2.00 (dq, 2H, $J = 11.9$ Hz, 7.5 Hz, $SCH_2$Me), 2.02 (dq, 2H, $J = 11.9$ Hz, 7.5 Hz, $SCH_2$Me), 2.47 (q, 2H, $J = 7.3$ Hz, $SCH_2$Me), 4.61 (m, 2H, $\eta^5$-$C_9H_7$), 4.68 (d, 2H, $J = 2.5$ Hz, $\eta^5$-$C_9H_7$), 4.69 (m, 2H, $\eta^5$-$C_9H_7$), 4.91 (t, 1H, $J = 2.5$ Hz, $\eta^5$-$C_9H_7$), 4.94 (t, 2H, $J = 2.5$ Hz, $\eta^5$-$C_9H_7$), 6.90–7.49 (m, 12H, aryl). Anal. Calc. for $C_{33}H_{36}S_3Ru_3$: C, 47.64; H, 4.36. Found: C, 47.91; H, 4.54.

### 3.4. Preparation of [($\eta^5$-$C_9H_7$)$_3$$Ru_3$($\mu$-SEt)$_2$($\mu$-SEtMe)][I] (**4a**)

To a solution of **2** (1.00 g, 1.20 mmol) in THF (30 ml) was added MeI (0.570 g, 3.94 mmol), and the

mixture was stirred at 50°C for 20 h. During this period the initial dark purple solution turned to a dark brown suspension. The solvent was removed in vacuo, and the residue was washed with benzene and dissolved in $CH_2Cl_2$. Addition of hexane to the $CH_2Cl_2$ solution gave **4a** as a dark brown powder (985 mg, 1.01 mmol, 84%), whose $^1$H-NMR analysis indicated that it contains no $CH_2Cl_2$ molecule. Crystalline samples of **4a**·$CH_2Cl_2$ for X-ray diffraction study and elemental analysis were obtained by slow diffusion of hexane into a $CH_2Cl_2$ solution of **4a**. A similar reaction at room temperature for 3 days also gave **4a** in 66% yield. $^1$H-NMR ($CDCl_3$): $\delta$ 0.62 (t, 3H, $J=7.3$ Hz, MeSCH$_2$*Me*), 1.22 (t, 6H, $J=7.3$ Hz, SCH$_2$*Me*), 2.25 (m, 4H, S*CH*$_2$Me), 2.51 (q, 2H, $J=7.3$ Hz, MeS*CH*$_2$Me), 2.94 (s, 3H, $SCH_3$), 4.50 (m, 2H, $\eta^5$-$C_9H_7$), 4.55 (t, 2H, $J=2.6$ Hz, $\eta^5$-$C_9H_7$), 5.23 (d, 2H, $J=2.6$ Hz, $\eta^5$-$C_9H_7$), 5.79 (t, 1H, $J=2.6$ Hz, $\eta^5$-$C_9H_7$), 5.97 (m, 2H, $\eta^5$-$C_9H_7$), 7.25-7.47 (m, 10H, aryl), 7.97 (d, 2H, $J=8.6$ Hz, aryl). Anal. Calc. for $C_{35}H_{41}S_3Cl_2Ru_3I$: C, 39.70; H, 3.90. Found: C, 40.01; H, 3.85.

### 3.5. Preparation of [($\eta^5$-$C_9H_7$)$_3$Ru$_3$($\mu$-SEt)$_2$($\mu$-SEtMe)][$PF_6$] (4b)

To a solution of **4a** (271 mg, 0.278 mmol) in $CH_2Cl_2$ (40 ml) was added $KPF_6$ (517 mg, 2.81 mmol), and the mixture was stirred at room temperature for 1 week. The solvent was removed in vacuo, and the resulting dark brown solid was extracted with $CH_2Cl_2$. Addition of hexane to the concentrated extract gave **4b**·$CH_2Cl_2$ as black crystals (240 mg, 0.223 mmol, 80%). $^1$H-NMR ($CDCl_3$): $\delta$ 0.61 (t, 3H, $J=6.9$ Hz, MeSCH$_2$*Me*), 1.22 (t, 6H, $J=7.6$ Hz, SCH$_2$*Me*), 2.24 (m, 4H, S*CH*$_2$Me), 2.51 (q, 2H, $J=6.9$ Hz, MeS*CH*$_2$Me), 2.62 (s, 3H, $SCH_3$), 4.46 (m, 2H, $\eta^5$-$C_9H_7$), 4.50 (t, 2H, $J=2.3$ Hz, $\eta^5$-$C_9H_7$), 5.20 (d, 2H, $J=2.3$ Hz, $\eta^5$-$C_9H_7$), 5.25 (m, 2H, $\eta^5$-$C_9H_7$), 5.79 (t, 1H, $J=2.3$ Hz, $\eta^5$-$C_9H_7$), 7.29–7.51 (m, 10H, aryl), 7.69 (d, 2H, $J=8.6$ Hz, aryl). Anal. Calc. for $C_{35}H_{41}F_6PS_3Cl_2Ru_3$: C, 39.03; H, 3.84. Found: C, 39.36; H, 3.88.

### 3.6. Preparation of [($\eta^5$-$C_9H_7$)$_2$Ru$_2$($\mu$-SEt)(CO)$_4$][$PF_6$] (5)

CO gas was bubbled into a solution of **4b** (58.0 mg, 0.0539 mmol) in $CH_2ClCH_2Cl$ (10 ml) at room temperature for 30 min and the solution was further stirred at 50°C under a CO atmosphere for 55 h. During this period the color of the solution changed from dark brown to orange. The solvent was removed in vacuo, and the resulting solid was washed with benzene and recrystallized from $CH_2Cl_2$-ether to give **5** as orange crystals (13.7 mg, 0.0183 mmol, 34%). IR (KBr disk, $cm^{-1}$): 1991, 2010, 2037, 2058 [$\nu$(CO)]. $^1$H-NMR ($C_6D_6$): $\delta$ 0.63 (t, 3H, $J=7.3$ Hz, SCH$_2$*Me*), 1.64 (q, 2H, $J=7.3$ Hz, S*CH*$_2$Me), 5.87 (m, 6H, $\eta^5$-$C_9H_7$), 7.47–7.62 (m, 8H, aryl). Anal. Calc. for $C_{24}H_{19}O_4F_6PSRu_2$: C, 38.41; H, 2.55. Found: C, 38.21; H, 2.82.

### 3.7. Preparation of [($\eta^5$-$C_9H_7$)$_3$Ru$_3$($\mu$-SEt)$_3$($\mu$-CO)(CO)] (6) and [($\eta^5$-$C_9H_7$)Ru($\mu$-SEt)(CO)]$_2$ (7)

CO gas was bubbled into a solution of **2** (0.203 g, 0.244 mmol) in THF (7 ml) for 15 min and the solution was further stirred under a CO atmosphere for 1 h at room temperature. During this period the color of the solution changed from dark purple to brown. After removal of the solvent under reduced pressure, the resulting solid was dissolved in benzene and loaded on an activated alumina column. The first reddish yellow band eluted with benzene and the second dark red band eluted with THF were collected. Each fraction was dried up, and the resulting solids were recrystallized from benzene-MeOH to give **7** as red crystals (44 mg, 0.0720 mmol, 20%) and **6** as black crystals (70 mg, 0.0789 mmol, 32%), respectively. **6**: IR (KBr disk, $cm^{-1}$): 1748, 1927 [$\nu$(CO)]. $^1$H-NMR ($C_6D_6$): $\delta$ 1.09 (t, 6H, $J=7.4$ Hz, SCH$_2$*Me*), 1.29 (t, 3H, $J=7.4$ Hz, SCH$_2$*Me*), 1.64 (dq, 2H, $J=12.8$, 7.4 Hz, S*CH*$_2$Me), 2.25 (q, 2H, $J=7.4$ Hz, S*CH*$_2$Me), 2.43 (dq, 2H, $J=12.8$, 7.4 Hz, S*CH*$_2$Me), 4.41 (m, 2H, $\eta^5$-$C_9H_7$), 5.07 (t, 2H, $J=2.6$ Hz, $\eta^5$-$C_9H_7$), 5.08 (t, 1H, $J=2.6$ Hz, $\eta^5$-$C_9H_7$), 5.24 (d, 2H, $J=2.6$ Hz, $\eta^5$-$C_9H_7$), 5.55 (m, 2H, $\eta^5$-$C_9H_7$), 6.75–7.38 (m, 12H, aryl). Anal. Calc. for $C_{35}H_{36}O_2S_3Ru_3$: C, 47.34; H, 4.09. Found: C, 47.06; H, 3.95. **7**: IR (KBr disk, $cm^{-1}$): 1896, 1923 [$\nu$(CO)]. $^1$H-NMR ($C_6D_6$): $\delta$ 1.05 (t, 6H, $J=7.3$ Hz, SCH$_2$*Me*), 2.54 (q, 4H, $J=7.3$ Hz, S*CH*$_2$Me), 4.39 (t, 2H, $J=2.5$ Hz, $\eta^5$-$C_9H_7$), 4.72 (d, 4H, $J=2.5$ Hz, $\eta^5$-$C_9H_7$), 6.93–7.20 (m, 8H, aryl). Anal. Calc. for $C_{24}H_{24}O_2S_2Ru_2$: C, 47.20; H, 3.96. Found C, 47.13; H, 4.03.

### 3.8. Preparation of [($\eta^5$-$C_5H_2$)Ru($\mu$-SEt)]$_3$ (8)

To a solution of [($\eta^5$-$C_5H_2$)RuCl($PPh_3$)$_2$] (1.00 g, 1.38 mmol) in THF (70 ml) was added NaSEt (0.41 g, 4.88 mmol), and the mixture was allowed to reflux for 15 min. Rapid color change from yellow to reddish brown was observed. The solvent was removed in vacuo, and the resulting solid was extracted with toluene. The extract was dried up, and the residue was recrystallized from THF-MeOH to give [($\eta^5$-$C_5H_2$)Ru(SEt)($PPh_3$)$_2$] as a red crystalline solid (0.406 g, 0.541 mmol, 39%). $^1$H-NMR ($C_6D_6$): $\delta$ 1.63 (t, 3H, $J=7.3$ Hz, SCH$_2$*Me*), 2.46 (q, 2H, $J=7.3$ Hz, S*CH*$_2$Me), 4.40 (s, 5H, $\eta^5$-$C_5H_2$), 6.97–7.84 (m, 30H, aryl); $^{31}$P{$^1$H}-NMR ($C_6D_6$): $\delta$ 41.57 (s). Anal. Calc. for $C_{43}H_{40}P_2SRu$: C, 68.69; H, 5.36. Found: C, 68.67; H, 5.58.

A red solution of [($\eta^5$-$C_5H_2$)Ru(SEt)($PPh_3$)$_2$] (1.23 g, 1.63 mmol) in toluene (50 ml) was allowed to reflux for 6 h. The brown solid obtained by evaporation of the

Table 5
X-ray crystallographic data for **4a**·$CH_2Cl_2$, **5**, **6**, and **7**

| | **4a**·$CH_2Cl_2$ | **5** | **6** | **7** |
|---|---|---|---|---|
| Formula | $C_{35}H_{41}S_3Cl_2Ru_3I$ | $C_{24}H_{19}O_4F_6PSRu_2$ | $C_{35}H_{36}O_2S_3Ru_3$ | $C_{24}H_{24}O_2S_2Ru_2$ |
| Molecular weight | 1058.91 | 750.58 | 888.06 | 610.71 |
| Space group | $P2_1/c$ | $P2_1/a$ | $P\bar{1}$ | $C2/c$ |
| Crystal system | Monoclinic | Monoclinic | Triclinic | Monoclinic |
| Crystal color | Dark brown | Orange | Black | Orange |
| Crystal dimensions (mm) | $0.25\times0.25\times0.30$ | $0.20\times0.30\times0.30$ | $0.20\times0.20\times0.80$ | $0.30\times0.60\times0.30$ |
| $a$ (Å) | 11.099(3) | 14.319(2) | 11.010(2) | 16.811(3) |
| $b$ (Å) | 27.569(4) | 12.223(2) | 17.203(2) | 10.594(3) |
| $c$ (Å) | 12.862(4) | 15.622(1) | 19.829(3) | 28.392(5) |
| $\alpha$ (°) | | | 107.756(9) | |
| $\beta$ (°) | 107.78(2) | 101.007(8) | 103.401(9) | 110.10(2) |
| $\gamma$ (°) | | | 99.745(9) | |
| V (Å$^3$) | 3747(1) | 2683.8(6) | 3360.5(9) | 4717(1) |
| Z | 4 | 4 | 4 | 8 |
| $D_{calc.}$ (g cm$^{-1}$) | 1.877 | 1.857 | 1.755 | 1.720 |
| $F(000)$ | 2072 | 1472 | 1768 | 2432 |
| $\mu$(Mo–K$_\alpha$) (cm$^{-1}$) | 23.52 | 13.34 | 15.48 | 14.76 |
| $2\theta$ range (°) | $5<2\theta<50$ | $5<2\theta<55$ | $5<2\theta<50$ | $5<2\theta<50$ |
| Scan speed (° min$^{-1}$) | 32 | 32 | 32 | 32 |
| Number of unique reflections | 6747 | 6459 | 11825 | 4725 |
| Transmission factors | 0.77–1.00 | 0.84–1.00 | 0.91–1.00 | 0.81–1.00 |
| Number of reflections used [$I>3\sigma(I)$] | 4237 | 3136 | 9405 | 3116 |
| Number of variables | 397 | 347 | 776 | 281 |
| $R$[a] | 0.038 | 0.051 | 0.026 | 0.034 |
| $R_w$[b] | 0.027 | 0.036 | 0.020 | 0.026 |
| GOF[c] | 1.52 | 2.04 | 2.08 | 2.12 |
| Maximum residual density, e Å$^{-3}$ | 0.84 | 0.69 | 0.77 | 0.57 |

[a] $R=\Sigma\|\|F_o|-|F_c\|/\Sigma|F_o|$.
[b] $R_w=[\Sigma w(|F_o|-|F_c|)^2/\Sigma wF_o^2]^{1/2}$, $w=1/\sigma^2(F_o)$.
[c] $\mathrm{GOF}=[\Sigma w(|F_o|-|F_c|)^2/(N_{obs}-N_{params})]^{1/2}$.

solvent under reduced pressure was dissolved in toluene/hexane (1/1) and loaded on an activated alumina column. The column was washed with toluene/hexane (1/1) to remove $PPh_3$, and then the reddish yellow band eluted with THF/hexane (1/1) was collected. The eluate was dried up, and the residue was extracted with benzene/hexane (1/1). The solvent was removed in vacuo, and the resulting solid was recrystallized from THF-hexane to give **8** as dark brown crystals (0.251 g, 0.368 mmol, 68%). $^1$H-NMR ($C_6D_6$): $\delta$ 1.12 (t, 6H, $J=7.3$ Hz, $SCH_2\mathit{Me}$), 1.28 (m, 4H, $S\mathit{CH_2}Me$), 1.55 (t, 3H, $J=7.3$ Hz, $SCH_2\mathit{Me}$), 3.52 (q, 2H, $J=7.3$ Hz, $S\mathit{CH_2}Me$), 4.58 (s, 10H, $\eta^5$-$C_5H_2$), 4.61 (s, 5H, $\eta^5$-$C_5H_2$). Anal. Calc. for $C_{21}H_{30}S_3Ru_3$: C, 36.99; H, 4.43. Found: C, 37.06; H, 4.58.

### 3.9. Preparation of $[(\eta^5\text{-}C_9H_7)Ru(SEt)Cl]_n$ (9)

A solution of **2** (499 mg, 0.600 mmol) in $CHCl_3$ (35 ml) was heated under reflux for 4 h. Rapid color change from purple to brown was observed. The brown solid obtained by evaporation of the solvent under reduced pressure was dissolved in THF and loaded on an activated alumina column. The reddish brown band eluted with THF was collected. The eluate was dried up, and the residue was recrystallized from acetone-hexane to give **9** as brown powder (76.2 mg, 14%). $^1$H-NMR ($CDCl_3$): $\delta$ 1.07 (t, 3H, $J=7.4$ Hz, $SCH_2\mathit{Me}$), 2.41 (q, 2H, $J=7.4$ Hz, $S\mathit{CH_2}Me$), 4.35 (t, 1H, $J=2.3$ Hz, $\eta^5$-$C_9H_7$), 5.31 (d, 2H, $J=2.3$ Hz, $\eta^5$-$C_9H_7$), 7.49–7.54 (m, 2H, aryl), 7.64–7.68 (m, 2H, aryl). Anal. Calc. for $C_{11}H_{12}SClRu$: C, 42.24; H, 3.87; S, 10.25; Cl, 11.33. Found: C, 41.73; H, 3.87; S, 10.04; Cl, 11.93.

### 3.10. X-ray crystallographic studies

Single crystals of **4a**·$CH_2Cl_2$, **5**, **6**, and **7** were sealed in glass capillaries under an argon atmosphere and used for data collection. Diffraction data were collected on a Rigaku AFC7R four-circle automated diffractometer with graphite-monochromatized Mo–K$_\alpha$ radiation ($\lambda=0.71069$ Å) at room temperature using the $\omega$-$2\theta$ scan technique for **4a**·$CH_2Cl_2$ and **5**, **6**, and **7**. The orientation matrices and unit cell parameters were determined by least-squares refinement of 25 machine cantered reflections with $30.7°<2\theta<39.9°$ for **4a**·$CH_2Cl_2$, $28.9°<2\theta<29.9°$ for **5**, $39.8°<2\theta<40.0°$ for **6**, and $22.3°<2\theta<24.4°$ for **7**. Intensity data were corrected for Lorentz and polarization effects and for

absorption (empirical, Ψ scans). For all crystals, no significant decay was observed for three standard reflections monitored every 150 reflections during the data collection.

The structure solution and refinements were carried out by using the teXsan crystallographic software package [22]. The positions of the non-hydrogen atoms were determined by Patterson methods (DIRDIF PATTY) [23] and subsequent Fourier syntheses. All non-hydrogen atoms were refined by full-matrix least-squares techniques with anisotropic thermal parameters. Hydrogen atoms were placed at the calculated positions and were included in the final stage of the refinement with fixed isotropic parameters. In the structure refinement of **7**, one of the SEt groups was found to be disordered. Two methyl carbon atoms attached to C(21) in the SEt group were placed at the two disordered positions and refined as C(22) and C(25) with 0.667 and 0.333 occupancies, respectively. Details of the X-ray diffraction study are summarized in Table 5.

## 4. Supplementary material available

Tables of atomic coordinates, anisotropic temperature factors of non-hydrogen atoms, and extensive bond distances and angles for **4a**·$CH_2Cl_2$, **5**, **6**, and **7** (54 pages) as well as listings of observed and calculated structure factors for **4a**·$CH_2Cl_2$, **5**, **6**, and **7** (137 pages) are available from M.H. upon request.

## Acknowledgements

This work was supported by a Grant-in-aid for Specially Promoted Research (09102004) from the Ministry of Education, Science, Sports, and Culture, Japan.

## References

[1] (a) P. Mathur, Adv. Organomet. Chem. 41 (1997) 243. (b) I. Dance, K. Fisher, Prog. Inorg. Chem. 41 (1994) 637. (c) T. Saito, in: M.H. Chisholm (Ed.), Early Transition Metal Clusters with π-Donor Ligands, VCH, New York, 1995, chapter 3. (d) T. Shibahara, Coord. Chem. Rev. 123 (1993) 73. (e) B. Krebs, G. Henkel, Angew. Chem., Int. Ed. Engl. 30 (1991) 769. (f) R.H. Holm, S. Ciurli, J.A. Weigel, Prog. Inorg. Chem. 38 (1990) 1.

[2] (a) D.C. Rees, M.K. Chan, J. Kim, Adv. Inorg. Chem. 40 (1994) 89. (b) D. Coucouvanis, in: E.I. Stiefel, D. Coucouvanis, W.E. Newton, (Eds.), Molybdenum Enzymes, Cofactors, and Model Systems, American Chemical Society, Washington, DC, 1993, p. 304.

[3] (a) R.J. Angelici, Acc. Chem. Res. 21 (1988) 387. (b) J. Chen, L.M. Daniels, R.J. Angelici, J. Am. Chem. Soc. 112 (1990) 199. (c) B.C. Wiegand, C.M. Friend, Chem. Rev. 92 (1992) 491. (d) V. Riaz, O.J. Curnow, M.D. Curtis, J. Am. Chem. Soc. 116 (1994) 4357. (e) C. Bianchini, A. Meli, J. Chem. Soc., Dalton Trans. (1996) 801.

[4] (a) M. Hidai, Y. Mizobe, H. Matsuzaka, J. Organomet. Chem. 473 (1994) 1. (b) M. Hidai, Y. Mizobe, in: E.I. Stiefel, K. Matsumoto (Eds.), Transition Metal Sulfur Chemistry: Biological and Industrial Significance, ACS Symposium Series 653, American Chemical Society, Washington, DC, 1996, p. 310.

[5] (a) M. Hidai, K. Imagawa, G. Cheng, Y. Mizobe, Y. Wakatsuki, H. Yamazaki, Chem. Lett. (1986) 1299. (b) S. Dev, Y. Mizobe, M. Hidai, Inorg. Chem. 29 (1990) 4797.

[6] (a) S. Dev, K. Imagawa, Y. Mizobe, G. Cheng, Y. Wakatsuki, H. Yamazaki, M. Hidai, Organometallics 8 (1989) 1232. (b) K. Hashizume, Y. Mizobe, M. Hidai, Organometallics 15 (1996) 3303.

[7] A. Takahashi, Y. Mizobe, H. Matsuzaka, S. Dev, M. Hidai, J. Organomet. Chem. 456 (1993) 243.

[8] (a) H. Matsuzaka, Y. Takagi, M. Hidai, Organometallics 13 (1994) 13. (b) M. Nishio, H. Matsuzaka, Y. Mizobe, T. Tanase, M. Hidai, Organometallics 13 (1994) 4214. (c) A. Takahashi, Y. Mizobe, T. Tanase, M. Hidai, J. Organomet. Chem. 496 (1995) 109. (d) M. Nishio, H. Matsuzaka, Y. Mizobe, M. Hidai, Organometallics 15 (1996) 965. (e) Y. Mizobe, M. Hosomizu, Y. Kubota, M. Hidai, J. Organomet. Chem. 507 (1996) 179. (f) Y. Takagi, H. Matsuzaka, Y. Ishii, M. Hidai, Organometallics 16 (1997) 4445.

[9] (a) S. Kuwata, Y. Mizobe, M. Hidai, Inorg. Chem. 33 (1994) 3619. (b) H. Shimada, J. Qü, H. Matsuzaka, Y. Ishii, M. Hidai, Chem. Lett. (1995) 671. (c) H. Matsuzaka, Y. Takagi, Y. Ishii, M. Nishio, M. Hidai, Organometallics 14 (1995) 2153. (d) Y. Nishibayashi, M. Yamanashi, Y. Takagi, M. Hidai, Chem. Commun. (1997) 859.

[10] For example (a) A. Venturelli, T.B. Rauchfuss, A.K. Verma, Inorg. Chem. 36 (1997) 1360. (b) Q. Feng, T.B. Rauchfuss, S.R. Wilson, J. Am. Chem. Soc. 117 (1995) 4702. (c) U. Koelle, C. Rietmann, J. Tjoe, T. Wagner, U. Englert, Organometallics 14 (1995) 703.

[11] (a) J.M. O'Connor, C.P. Casey, Chem. Rev. 87 (1987) 307. (b) M.E. Rerek, L.-N. Ji, F. Basolo, J. Chem. Soc., Chem. Commun. (1983) 1208.

[12] (a) M. Bassetti, P. Casellato, M.P. Gamasa, J. Gimeno, C. González-Bernardo, B. Martín-Vaca, Organometallics 16 (1997) 5470. (b) M.C. Comstock, J.R. Shapley, Organometallics 16 (1997) 4816. (c) L.P. Szajek, J.R. Shapley, Organometallics 13 (1994) 1395, and references therein.

[13] (a) M.C. Comstock, S.R. Wilson, J.R. Sharpley, Organometallics 13 (1994) 3805. (b) C. Bonifaci, G. Carta, A. Ceccon, A. Gambaro, S. Santi, A. Venzo, Organometallics 15 (1996) 1630. (c) L. Mantovani, A. Ceccon, A. Gambaro, S. Santi, P. Ganis, A. Venzo, Organometallics 16 (1997) 2682.

[14] A. Shaver, P.-Y. Plouffe, D.C. Liles, E. Singleton, Inorg. Chem. 31 (1992) 997.

[15] M. Nishio, Y. Mizobe, H. Matsuzaka, M. Hidai, Inorg. Chim. Acta 265 (1997) 59.

[16] S.A. Westcott, A.K. Kakkar, G. Stringer, N.J. Taylor, T.B. Marder, J. Organomet. Chem. 394 (1990) 777.

[17] S.D. Killops, S.A.R. Knox, J. Chem. Soc., Dalton Trans. (1978) 1260.

[18] A. Hörnig, C. Rietmann, U. Englert, T. Wagner, U. Kölle, Chem. Ber. 126 (1993) 2609.

[19] R. Büchner, J.S. Field, R.J. Haines, J. Chem. Soc., Dalton Trans. (1996) 3533.

[20] L.A. Oro, M.A. Ciriano, M. Campo, C. Foces-Foces, F.H. Cano, J. Organomet. Chem. 289 (1985) 117.

[21] M.I. Bruce, N.J. Windsor, Aust. J. Chem. 30 (1977) 1601.

[22] teXsan: Crystal Structure Analysis Package, Molecular Structure Corp., 1985 and 1992.

[23] PATTY: P.T. Beurskens, G. Admiraal, G. Beurskens, W.P. Bosman, S. Garcia-Granda, R.O. Gould, J.M.M. Smits, C. Smykalla, The DIRDIF program system, Technical Report of the Crystallography Laboratory, University of Nijmegen, Nijmegen, the Netherlands, 1992.